J. Fluid Mech. (2003), *vol.* 482, *pp.* 1–15.
DOI: 10.1017/S0022112003003847 Printed in the United Kingdom

On the instability of Stokes layers at high Reynolds numbers

By PHILIP HALL

Department of Mathematics, Imperial College of Science, Technology and Medicine, London SW7 2BZ, UK

(Received 11 March 2002 and in revised form 25 November 2002)

The inviscid instability of Stokes layers is investigated. The Stokes layer is shown to support inviscid Floquet modes at sufficiently high values of the disturbance wavenumbers. Other non-Floquet modes are investigated and are shown to be the likely cause for instability in Stokes layers. These modes intersect with a viscous continuous spectrum of disturbances and it is this interaction which enables free-stream disturbances to penetrate into the boundary layer and amplify exponentially. The relevance of the inviscid theory to previous viscous instability calculations for Stokes layers is discussed.

1. Introduction

The Stokes layer induced by a rigid wall oscillating transversely in a viscous fluid is one of the few exact solutions of the unsteady Navier–Stokes equations. For a general unsteady flow, the concept of instability is only well defined if the flow varies slowly in time. However, if the unsteady flow is periodic in time we can use Floquet theory to give a clear definition of what we mean by instability. In the situation where the unsteady flow varies slowly and is also periodic then the stability problem can be tackled by both Floquet and local (WKB) methods. The Stokes layer at high values of the Reynolds number is one such flow and it is that limit with which we concern ourselves here. The relationship, if any, between local and Floquet modes is a major part of this investigation.

The first investigation of the Stokes layer instability problem is due to von Kerczek & Davis (1974) who, for computational reasons, introduced a second boundary located several Stokes layer thicknesses away from the moving wall. No unstable modes were found at Reynolds numbers up to about 400. Hall (1978) investigated the problem in a semi-infinite fluid layer using the method of Seminara & Hall (1975) and found no unstable modes up to Reynolds numbers of about 160. The stable modes found by Hall were found to exist only over finite ranges of the wavenumber and the modes entered the continuous spectrum at the endpoints of these ranges.

It has been known for a long time (von Kerczek & Davis 1974; Cowley 1987) that the instantaneous profiles of a Stokes boundary layer can be massively unstable at Reynolds numbers at which there are no unstable Floquet modes. Cowley (1987) investigated the problem at high Reynolds numbers and found various unstable eigenvalues of the instantaneous Rayleigh equation which is the leading-order approximation to the linear stability problem at high values of the Reynolds number. However, since the modes found by Cowley did not have growth rates periodic in time, none of his solutions could be used to construct Floquet modes. More

recently, Blennerhassett & Bassom (2002) extended the calculation of Hall (1978) to much higher Reynolds numbers and they conclude that the Stokes layer becomes linearly unstable at a Reynolds number of about 708. This extension is non-trivial because the method of Hall is essentially a power series solution in Reynolds number and Blennerhassett & Bassom (2002 hereinafter referred to as BB) needed to use 128 bit arithmetic in order to retain sufficient accuracy at numerically larger values of the Reynolds number. The neutral curve found by the latter authors is open in the wavenumber–Reynolds number plane which suggests that unstable Floquet modes should exist for larger Reynolds numbers. This apparent inconsistency between the results of these authors and those of Hall (1978) and Cowley (1987) is investigated here.

The procedure adopted in the rest of the paper is as follows. In § 2 we give a brief derivation of the inviscid eigenvalue problem and show how the local modes appropriate to this limit could in principle reduce to Floquet modes. In § 3 we discuss our numerical results obtained by solving the Rayleigh equation and discuss the 'birth' and 'death' of various modes. The role of free-stream disturbances is also discussed in that section. Finally, in § 4 we draw some conclusions.

2. Formulation of the stability problem

Our concern is with the instability of the flow adjacent to the fixed rigid wall defined by $y = 0$ when an oscillatory pressure gradient in the x-direction drives a unidirectional flow $-U_0 \cos \omega t$ at large distances from the wall. Here, ω is a frequency, t denotes time and if ν is the kinematic viscosity of the fluid then the velocity of the flow is given by

$$\boldsymbol{u} = U_0\{u_B(Y, T), 0\}, \quad u_B = \cos(T - Y)\mathrm{e}^{-Y} - \cos T,$$

where $T = \omega t$ and $(X, Y) = (x, y)/(2\nu/\omega)^{1/2}$. The Reynolds number for the flow is defined by

$$R = \frac{U_0\sqrt{2}}{\sqrt{\nu\omega}},$$

and we will be primarily concerned with the limit $R \to \infty$. We will only give a brief description of formulation of the instability problem here (see Hall 1978 for more details).

Following Hall (1978), it is easy to show that a perturbation to the above flow satisfies the unsteady Orr–Sommerfeld equation

$$\left.\begin{aligned} \left\langle u_B - \frac{2}{\mathrm{i}\alpha R}\frac{\partial}{\partial T}\right\rangle \langle \psi_{YY} - \alpha^2\psi\rangle - u_{BYY}\psi = \frac{1}{\mathrm{i}\alpha R}\left\langle \partial_Y^2 - \alpha^2\right\rangle^2\psi, \\ \psi = \psi_Y = 0, \quad Y = 0, \infty. \end{aligned}\right\} \tag{2.1}$$

Here, α is the wavenumber of the disturbance which we will assume to be real. The stream function ψ is a function of Y and T and Floquet solutions of (2.1) are of the form

$$\psi = \mathrm{e}^{\mu T}\widehat{\psi}(Y, T), \quad \widehat{\psi}(Y, T + 2\pi) = \widehat{\psi}(Y, T).$$

Hall (1978) found only stable Floquet solutions ($\mu_r < 0$), but recently BB, using exactly the same solution procedure as Hall (1978), found a finite band of unstable wavenumbers for R greater than about 708. The neutral curve found by BB is 'open' at the larger values of R used in their calculations so we would expect instability to

be present in the inviscid limit $R \to \infty$. The latter limit was investigated by Cowley (1987) who found local instabilities but no Floquet solutions of the problem. Our calculations complement those of Cowley and suggest the origin of the disturbances which are known experimentally to cause transition to turbulence in Stokes layers; see for example Clamen & Minton (1977).

For large Reynolds numbers, we seek a solution of (2.1) by writing

$$\psi = \left\{ \psi_0(Y, T) + \frac{1}{\sqrt{R}} \psi_1(Y, T) + \ldots \right\} \exp\left\{ \tfrac{1}{2} R \int^T \Omega(\tau)\, \mathrm{d}\tau \right\}, \tag{2.2}$$

where we have anticipated that viscous effects will drive the $O(1/\sqrt{R})$ term above and the factor of 2 in the exponential has been introduced for convenience. If we define $\Omega = -\mathrm{i}\alpha c\,(T)$ then the local wavespeed c, assumed to be complex, satisfies the Rayleigh instability problem

$$(u_B - c)(\psi_{0YY} - \alpha^2 \psi_0) - u_{BYY} \psi_0 = 0, \quad \psi_0 = 0, \quad Y = 0, \infty. \tag{2.3}$$

We note that if we can compute $c\,(T)$ as a continuous function of T over one period then it corresponds to a Floquet solution of (2.3) only if

$$c(T + 2\pi) = c(T),$$

and the Floquet exponent μ is then given by

$$\mu = \frac{-\mathrm{i}\alpha R}{4\pi} \int_0^{2\pi} c(T)\, \mathrm{d}T. \tag{2.4}$$

Cowley (1987), in his investigation of (2.3), was unable to locate such Floquet modes. The Rayleigh problem (2.3) must be solved numerically and, in order to navigate around any critical layers in the appropriate manner, we choose to integrate (2.3) in the complex plane along the contour defined by

$$\zeta = \theta + \mathrm{i}\gamma\theta u_B'(\theta) \quad (0 < \theta < \infty).$$

Here, a prime denotes differentiation with respect to θ and γ is a negative constant chosen for convenience. It was also found useful in cases where the eigenfunction is concentrated near the wall to work on a stretched grid defined by

$$\phi = \frac{2}{\pi} \tan^{-1} \theta \quad \text{with } 0 < \phi < 1.$$

If (2.3) is discretized using central differences on a uniform grid in θ or ϕ, we obtain a generalized eigenvalue problem of the form

$$(\boldsymbol{A} - c\boldsymbol{B})\boldsymbol{V} = 0. \tag{2.5}$$

The global spectrum of (2.5) was found using a NAG routine whilst individual eigenvalues were followed by augmenting (2.5) with

$$\frac{\mathrm{d}c}{\mathrm{d}\theta} = 0 \quad \text{or} \quad \frac{\mathrm{d}c}{\mathrm{d}\phi} = 0,$$

and using Newton iteration. The global spectrum calculated will contain both approximations (for a given grid size) to eigenvalues c of (2.3) and spurious eigenvalues associated with the discretization. The constant γ was taken to be -0.1 in most of the calculations, though for eigenfunctions concentrated near the wall, somewhat larger values of γ were used.

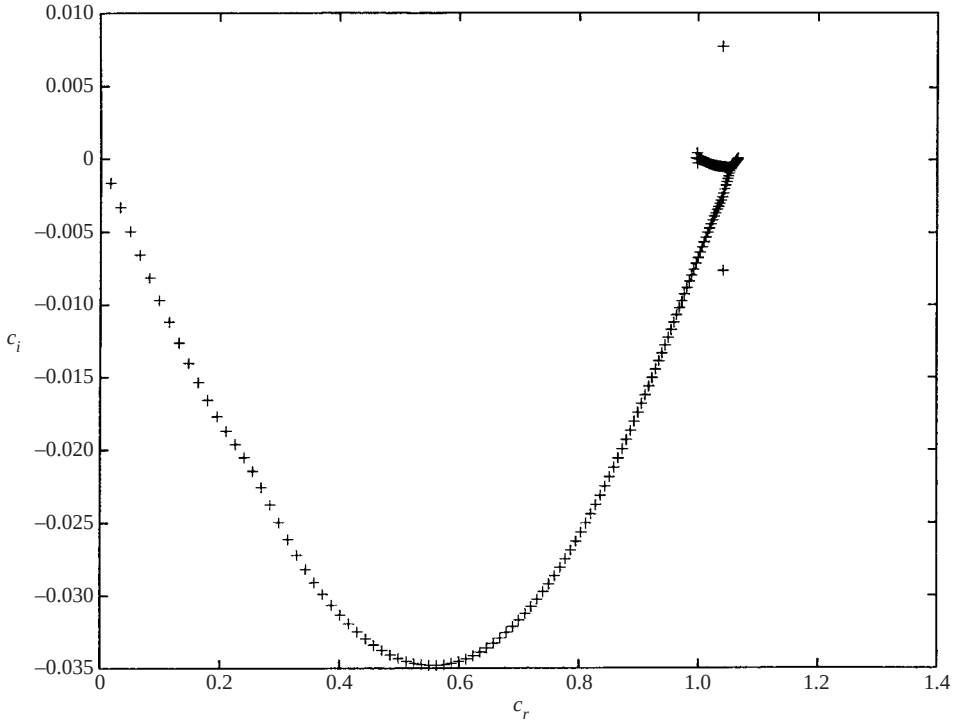

FIGURE 1. The global eigenvalue spectrum for $\alpha = 0.4$, $\gamma = -0.1$ and 600 grid points.

3. Results

Figure 1 shows the spectrum of (2.5) for the case $\alpha = 0.4, \gamma = -0.1, T = \pi$ and 600 grid points (on the unstretched grid), respectively, with 'infinity' taken to be 10. At this value of t, the free-stream speed is 1, so we note the apparently large number of eigenvalues which have the real part of c close to this value. Our calculations reproduced the results of Cowley (1987) where checks could be made. Cowley reported that for a critical value of α close to $\alpha = 0.53$, two eigenvalues coalesced. In fact, this value of α, which we hereinafter denote by α_c, delineates two distinct types of behaviour of the spectrum.

3.1. *The spectrum for* $0 < \alpha < \alpha_c$

In order to illustrate the behaviour of the spectrum in this regime we shall in the first instance concentrate on the case $\alpha = 0.2$. Figure 2 shows the wavespeed c_r and growth rate c_i for $\alpha = 0.2$ and $-\frac{3}{4}\pi < T < \pi$ of the mode corresponding to the single unstable mode of figure 1. Note that we could start our calculations with any of the discrete non-spurious modes of figure 1 since the modes will be seen to connect when time is varied. (See also figure 3 for the evolution of c_r and c_i with T.)When T decreases from π the disturbance becomes increasingly unstable until a maximum of the growth rate is achieved when $T \simeq 1$, after which the disturbance becomes stable. After a short interval of instability near $T \simeq -1.7$, the disturbance again becomes stable. When $T \rightarrow > -\frac{3}{4}\pi$, the real and imaginary parts of c approach zero and the disturbance becomes concentrated near the wall. In this limit, viscous effects become important and this will be discussed in more detail later. If T is increased from π, the growth rate

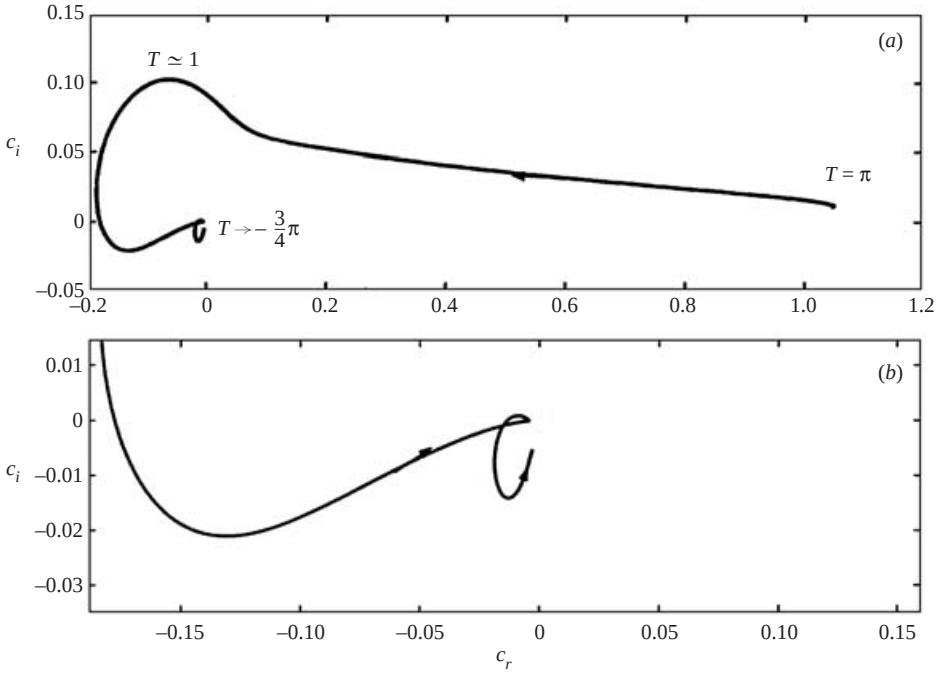

FIGURE 2. (*a*) The evolution of the eigenvalues of (2.5) for $\alpha = 0.2$. (*b*) The evolution near the origin of the eigenvalues of (2.5) for $\alpha = 0.2$.

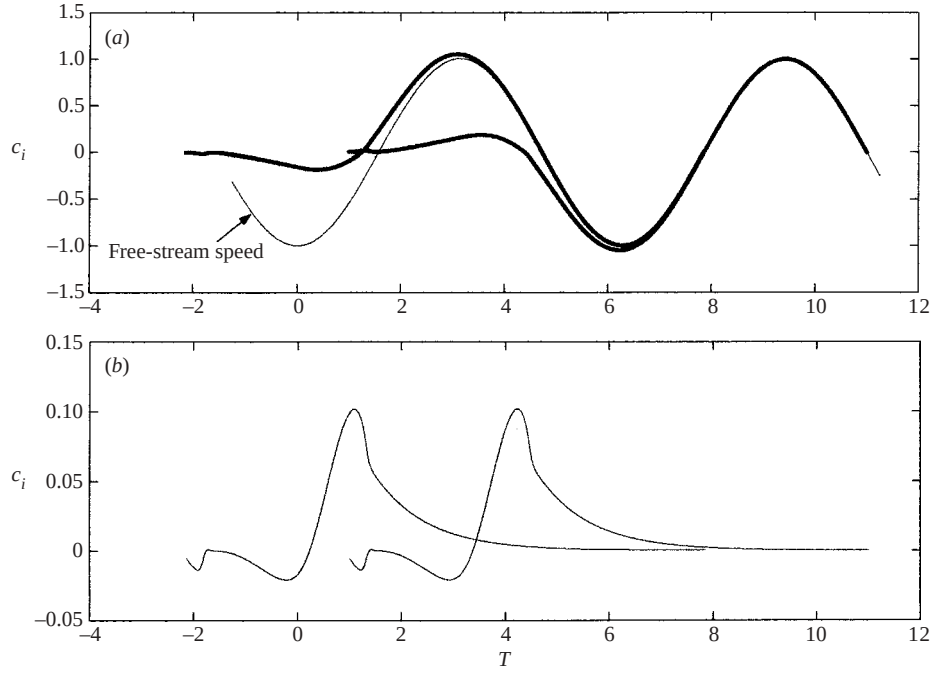

FIGURE 3. (*a*) The quantity c_r as a function of T for $\alpha = 0.2$. (*b*) The quantity c_r as a function of T for $\alpha = 0.2$.

decreases monotonically to zero whilst the wavespeed asymptotes to the free-stream speed. We also notice that, since $u_B(y, T) = u_B(y, T + 2\pi)$, $u_B(y, T) = -u_B(y, T + \pi)$, the results shown in figure 2 can be used to generate families of eigenvalues using the relationship $c(T + \pi) = -\bar{c}(T)$, $c(T + 2\pi) = c(T)$.

Using the above result, after first continuing the calculation of c for $T > \pi$, we construct figures 3(a) and 3(b) which show c_r and c_i over a range of values of t. The arrow shows the curve which defines the free-stream speed at each instant in time. The key features illustrated in this figure are:

(i) A stable eigenvalue emerges out of the origin in the complex c plane each time the wall shear vanishes (i.e. when $T = \frac{1}{4}\pi + n\pi$, $n = 0, \pm 1, \pm 2, \ldots$).

(ii) Each eigenvalue emerging from a time when the shear vanishes is initially stable, then has a small region of instability before ultimately becoming unstable for all time greater than a critical value.

(iii) The growth rate of any disturbance tends to zero from above for large times.

We also remark that for each eigenvalue the free-stream speed coincides with the wavespeed of the disturbance at just one value of T and that the growth rate is negative at these times. If we were solving the Orr–Sommerfeld equation, this would alert us to the possibility of a continuous spectrum, but the inviscid problem has no such spectrum. However, the inviscid problem must be thought of as the limit of the viscous one when $R \to \infty$, so the point requires further investigation. We will return to this matter later. Figure 3 shows that the mode emanating from $T = \frac{1}{4}\pi + n\pi, n = \pm 1, \pm 2, \ldots$ becomes the fastest growing mode over an interval of length π and remains unstable for large times but with an exponentially small growth rate. Thus, at large times, the mode might be relevant if transition is caused by free-stream disturbances, but otherwise in any time interval of length π, the mode emanating from the latest time when the wall shear vanished will dominate.

In figure 4, we show the eigenfunctions associated with some of the eigenvalues shown in figure 2. The eigenfunctions shown have been normalized by their maximum absolute value. We observe that the eigenfunctions are initially located near the wall and then drift outwards. Further increases in T show that the outward drift continues monotonically.

3.2. *The spectrum for* $\alpha > \alpha_c$

In figures 3(a) and 3(b), we can see that there are values of T, T_c and T_r, close to π and $\frac{1}{2}\pi$ when the two most unstable eigenvalues have their real or imaginary parts, respectively the same. When α is increased from 0.2, the times T_r and T_c approach each other and coalesce when $\alpha = \alpha_c \simeq 0.53$. The spectrum for $\alpha > \alpha_c$ then takes on a different form because of this coalescence of eigenvalues at $\alpha = \alpha_c$. The subsequent splitting of the eigenvalues leads to the generation of a Floquet mode with c now a periodic function of time. In addition, there remains a mode which originates at the wall each time the wall shear vanishes. This mode eventually becomes unstable but, like the modes for $\alpha < \alpha_c$, the growth rate of the modes tends to zero for large T and the wavespeed approaches the free-stream speed. We note, however, that the non-Floquet mode no longer intersects with what would be a continuous spectrum of the viscous problem.

Figures 5(a) and 5(b) show the quantities c_r and c_i for the Floquet and non-Floquet modes when $\alpha = 0.56$. Figures 5(c)–5(f) show the dependence of these quantities on time. The free-stream speed is also shown in figures 5(c) and 5(e). The eigenfunctions associated with the modes which originate when the wall shear vanishes are similar to those shown in figure 4 with the eigenfunction drifting further and further from

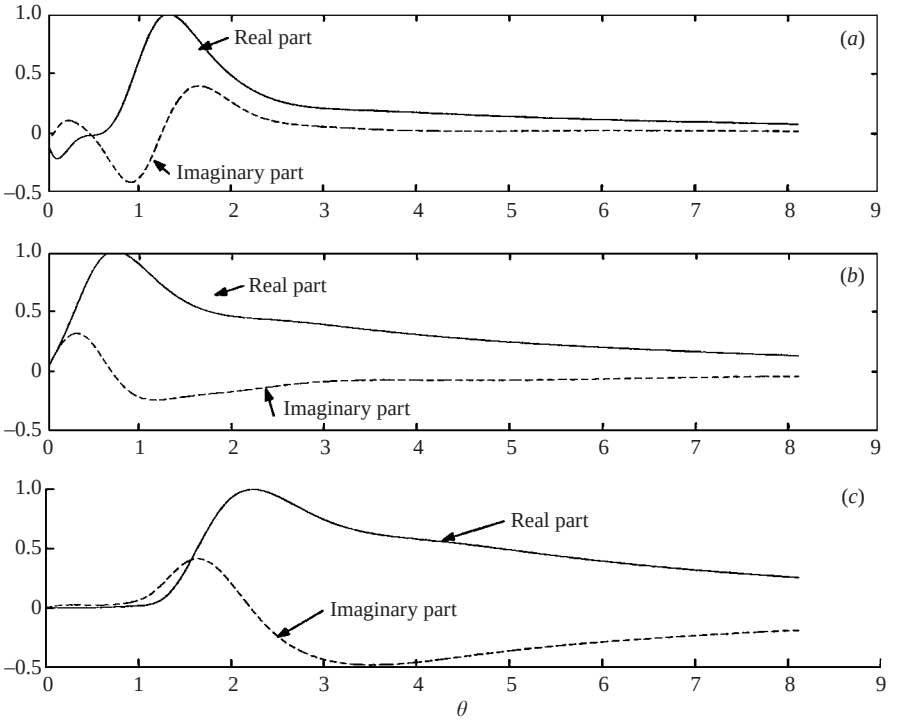

FIGURE 4. The eigenfunctions for $\alpha = 0.2$, (*a*) $T = -2$, (*b*) 0 and (*c*) 2.

the wall as T increases. The eigenfunctions associated with the Floquet mode are shown in figure 6, we see that this mode stays within the boundary layer.

The Floquet exponent of the Floquet mode is we recall defined by (2.4). Figure 7 shows μ_i/R as a function of α for $\alpha > \alpha_c$. We see that all the modes are stable and that the least stable mode has $\alpha = \alpha_c$.

The modes originating from $T = \frac{1}{4}\pi + n\pi$, n an integer, for any value of α do not, of course, form Floquet modes since c in this case is not a periodic function of T. However, for each such mode, we can define a 'lifetime growth' exponent defined by

$$G = -\int_{\pi/4}^{\infty} \mathrm{i}\alpha c_i(T)\,\mathrm{d}T.$$

(The integral converges since we shall see later that $c_i \to 0$ exponentially when $T \to \infty$). Note here that G is the same for any of the modes originating from $T = \frac{1}{4}\pi + n\pi$. Figure 8 shows G as a function of α for this type of mode. The mode which has the largest growth corresponds to $\alpha \simeq 0.25$ and we note that the modes for sufficiently large wavenumbers lead to no net growth. The above discussion suggests strongly that there are no unstable Floquet solutions of the Stokes layer instability problem at large R.

3.3. *The origin of the inviscid modes*

Now let us give a brief discussion about the nature of the 'birth' of the inviscid modes at $T = \frac{1}{4}\pi + n\pi$ and their large time behaviour. For definiteness, consider the mode which originates at $T = \frac{1}{4}\pi$ for a given value of α. In the neighbourhood of $T = \frac{1}{4}\pi$,

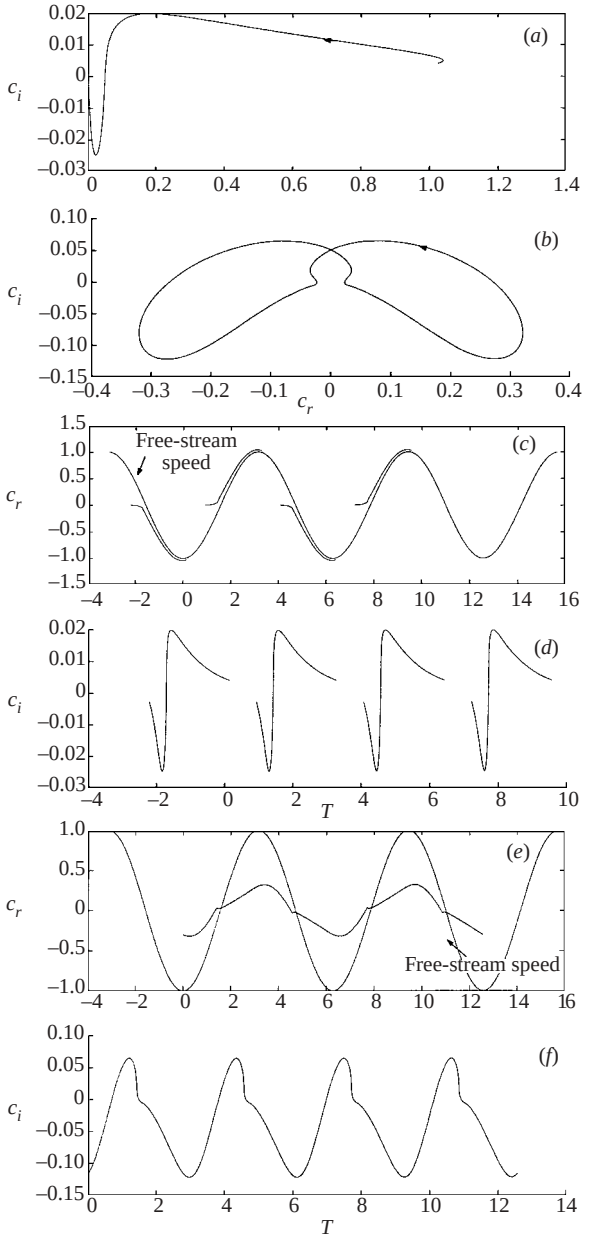

FIGURE 5. The eigenvalue for (*a*) the non-Floquet mode and (*b*) the Floquet mode when $\alpha = 0.56$. (*c*) The real part of c and (*d*) the imaginary part of c as functions of T for the non-Floquet mode when $\alpha = 0.56$. (*e*) The wavespeed of the Floquet mode when $\alpha = 0.56$. (*f*) The imaginary part of c for the Floquet mode when $\alpha = 0.56$.

the basic velocity profile near the wall takes the form

$$u_B = \sqrt{2}\left\{\left(T - \tfrac{1}{4}\pi\right) Y - \tfrac{1}{2}Y^2 + \ldots\right\}$$

so that there is flow reversal near the wall for $T \to \frac{1}{4}\pi_+$ and a monotonically decreasing profile near the wall for T slightly less than $\frac{1}{4}\pi$. It follows that viscous effects enter the

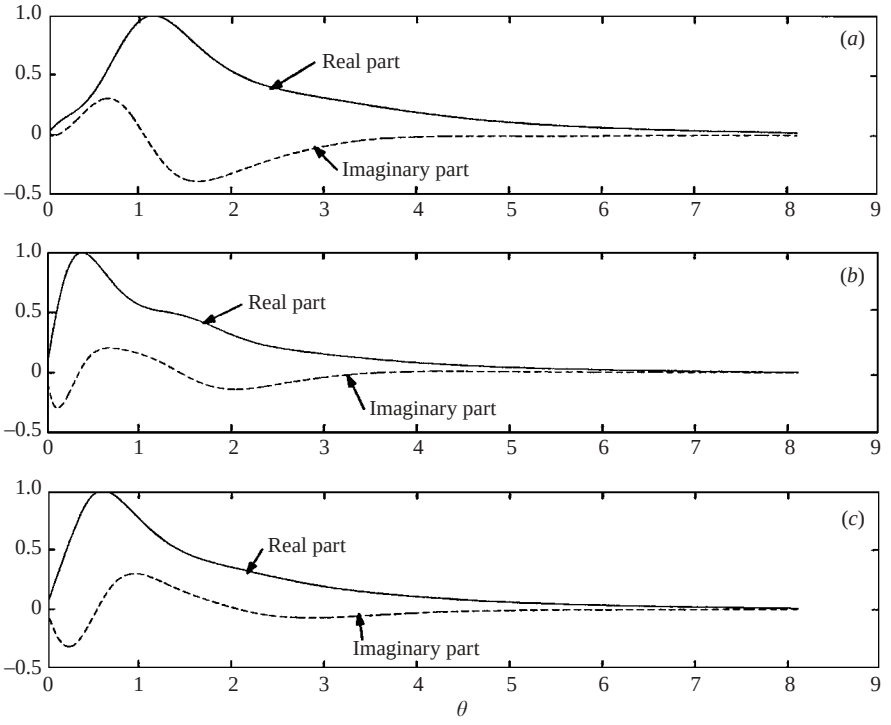

FIGURE 6. The eigenfunctions for $\alpha = 0.56$, (*a*) $T = 1$, (*b*) 2 and (*c*) 3.

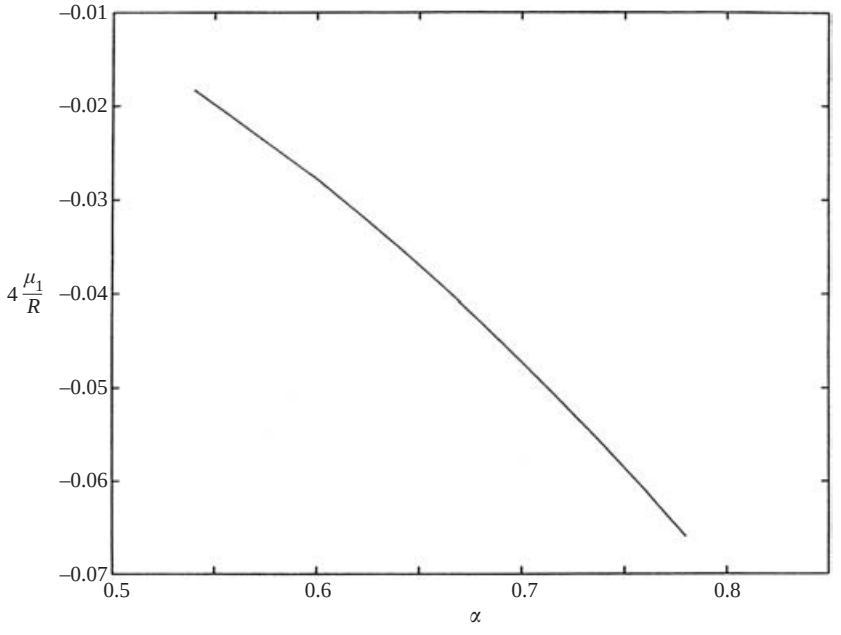

FIGURE 7. The Floquet exponent as a function of α.

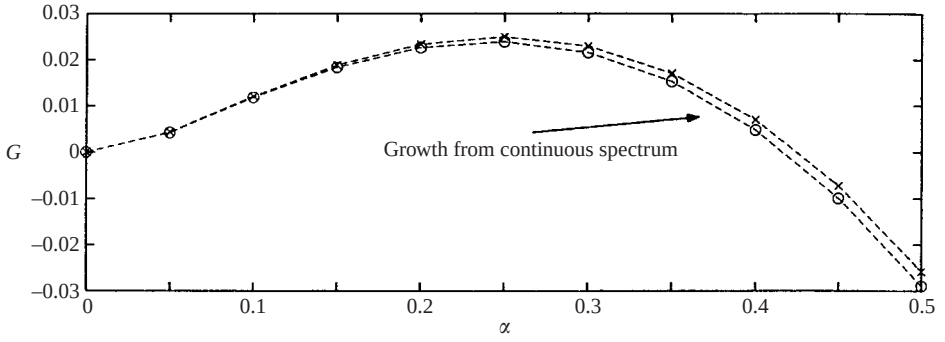

FIGURE 8. The 'lifetime growth' exponent G as a function of α.

problem for $T - \frac{1}{4}\pi = O(R^{-1/4})$, $Y = O(R^{-1/4})$ and that in this time regime c should be expanded as

$$c = R^{-1/2}c_1(\tau) + \ldots, \qquad \text{with } \tau = \left(T - \tfrac{1}{4}\pi\right) R^{1/4}.$$

The details of the above expansion are straightforward so we do not give them here. We note only that $c_1(\tau)$ above may be found to obtain a match with the inviscid solution when $\tau \to \infty$. Further, we note that $c_1 \sim |\tau|^{2/3}$ when $\tau \to -\infty$ so that c ultimately becomes $O(R^{-1/6})$, the wavespeed for a stable viscous wall mode. At later stages, critical layers away from the wall develop and the situation becomes more complex. The main point is that the mode remains viscous and stable and does not re-enter the inviscid spectrum.

3.4. *The end stages of the inviscid modes*

We have seen above that the modes which emerge from $T = \frac{1}{4}\pi + n\pi$ eventually become unstable for all time on the basis of inviscid theory and move further and further away from the wall whilst the wavespeed approaches the free-stream speed. Cowley (1987) has given an asymptotic structure for these modes, previously Tromans (1979) had suggested that they had exponentially small growth rates for large time. For large T, Cowley shows that

$$c = -\cos T + c_0 \exp\left[-T - 2n\pi\right] + \ldots$$

and

$$c = -\cos T - \bar{c}_0 \exp\left[-T - 2n\pi - \pi\right] + \ldots$$

where c_0 is a function of α with positive imaginary part and n is a large integer. The modes are concentrated in a layer of thickness $O(1)$ at a distance $|\log\epsilon|$ from the wall where

$$\log\epsilon^{-1} = 2n\pi + Y_0 \quad (0 \leqslant Y_0 \leqslant 2\pi).$$

The modes decay exponentially in amplitude in both directions away from the layer.

We expect that viscous effects associated with the boundary layer of thickness $R^{-1/2}$ at the wall will lead to $O(R^{-1/2})$ corrections to the growth rate, so we might anticipate that the modes will be ultimately stabilized. Here we have assumed that, as is the case for inviscid instabilities of steady flows, viscous effects are stabilizing. However, we should also note that, if the growth rate at leading order is tending to zero exponentially, the quasi-steady approximation will itself fail at large times.

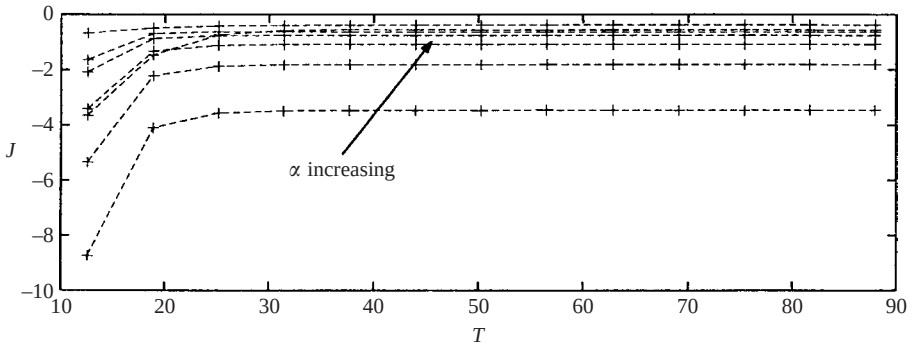

FIGURE 9. The growth rate J for $0 = 0.05, 0.1, 0.2, 0.3, 0.4, 0.5, 0.6$.

In particular, if $\exp[-T - 2n\pi] = O(1/R)$, then the WKB formulation fails and we return to a fully unsteady partial differential equation to describe the modes. We can derive the appropriate equation directly from (2.1). We write

$$T = |\log R| + s, |\log R| + \zeta = Y, \quad \psi = \exp\left(-\tfrac{1}{2}R\mathrm{i}\alpha \sin T\right)\Psi_0(\zeta, s) + \ldots,$$

substitute into (2.1) with Y replaced by $\zeta + \log R$ and retain leading-order times to give

$$\left(\widehat{u}(\zeta, s) - \frac{2}{\mathrm{i}\alpha}\frac{\partial}{\partial s}\right)(\Psi_{0\zeta\zeta} - a^2\Psi_0) - \widehat{u}_{\zeta\zeta}\Psi_0 = \frac{1}{\mathrm{i}\alpha}\left(\partial_\zeta^2 - \alpha^2\right)^2\Psi_0, \tag{3.1}$$

with $\widehat{u} = \cos(s - \zeta)\mathrm{e}^{-\zeta}$, which must be solved subject to

$$\Psi_0 \to 0, \quad |\zeta| \to \infty. \tag{3.2}$$

Thus, in a frame of reference moving with the free stream, we simply recover the original evolution equation extended to an infinite domain with Reynolds number of unity. If the limit $s \to -\infty$ is taken in (3.1) we can recover Cowley's large-time inviscid mode structure. Equations (3.1) and (3.2) will have Floquet solutions of the form

$$\Psi_0 = \mathrm{e}^{\eta s}\widehat{\Psi}_0(\zeta, s), \quad \widehat{\Psi}_0(\zeta, s + 2\pi) = \widehat{\Psi}_0(\zeta, s), \tag{3.3}$$

which could, in principle, be solved for using the method of Hall (1978). However, if such modes exist, they would emerge as the large s structure of an arbitrary disturbance imposed on the flow at some initial value of s. In order to investigate that possibility we integrated (3.1) using the numerical scheme of Hall (1983) subject to the conditions

$$\Psi_0 = 0, \quad |\zeta| \to \infty, \quad \Psi_0 = \beta(\zeta), \quad s = 0,$$

for some initial distribution $\beta(\zeta)$. In order to measure the growth or decay of Ψ_0 we computed

$$I(\alpha, s) = \int_{-\infty}^{\infty} |\Psi_0|^2 \,\mathrm{d}\zeta.$$

Figure 9 shows $J = \log(I(s = 2n\pi)/I(s = 2[n - 1]\pi))$ for different values of α with an initial perturbation $\beta(\zeta) = (1 + \sin\zeta)\mathrm{e}^{-\zeta^2}$. We see that for large s, J tends to a negative constant, indicating that the disturbance has taken on the form of a stable Floquet mode of (3.1). The calculation was repeated with different initial conditions and J was found to approach the same negative constant, We conclude that the

unstable modes which originate at the times when the wall shear vanishes, gradually move out towards the edge of the boundary layer where at large times their growth rates decay to zero and viscous effects come into play. In fact, the modes go through an interval where they are genuinely unsteady before emerging as stable Floquet solutions. These new Floquet modes are trapped outside the boundary layer and are not related to the Floquet solutions of figure 5.

3.5. *Inviscid modes and the continuous spectrum*

The inviscid problem (2.3) for large values of Y reduces to

$$\psi_{0YY} - \alpha^2 \psi_0 = 0,$$

so that, for real wavenumbers, α the disturbance necessarily decays exponentially and there can be no continuous spectrum. However, the inviscid modes do not satisfy the no-slip condition at $Y = 0$, so that if higher-order terms in (2.2) are retained then the possibility of a continuous spectrum will again exist.

Suppose then that we have a stable eigenmode of (2.5) and that the wavespeed of the mode is equal to the free-stream speed. Note that we have anticipated here the usual result that continuous spectrum modes are convected along with the free-stream speed outside the boundary layer. It is expected that viscous effects will produce an $O(R^{-1/2})$ correction to the wavespeed so we expand

$$c = c_0 + \frac{c_1}{R^{1/2}} + \ldots$$

and retain the expansion (2.2). At order $R^{-1/2}$, we find that ψ_1 satisfies

$$(u_B - c_0)(\psi_{1YY} - \alpha^2 \psi_1) - u_{BYY} \psi_1 = c_1 (\psi_{0YY} - \alpha^2 \psi_0). \tag{3.4}$$

Near the wall, we write

$$\varsigma = R^{1/2} Y,$$

and, since $\psi_0 = 0$, $Y = 0$, we replace (2.2) by

$$\psi = \left[\Psi_1 (\varsigma, T)\, R^{-1/2} + \ldots \right] \exp \left\{ \tfrac{1}{2} R \int^T \Omega (\tau)\, \mathrm{d}\tau \right\}.$$

The function Ψ_1 is then found to satisfy

$$-c_0 \Psi_{1\zeta\zeta} = \frac{1}{\mathrm{i}\alpha} \Psi_{1\zeta\zeta\zeta\zeta}, \quad \Psi_1 = \Psi_{1\zeta}, \quad \zeta = 0, \quad \Psi_1 \tilde{} \zeta\, \psi_{0Y} (0, T), \quad \zeta \to \infty.$$

Hence, Ψ_1 is given by

$$\Psi_1 = \psi_{0Y} (0, T) \left\{ \zeta + \frac{\exp(-\sqrt{\mathrm{i}J}\zeta)}{\sqrt{\mathrm{i}J}} - \frac{1}{\sqrt{\mathrm{i}J}} \right\},$$

with $J = J(T) = -\alpha c_0$. It follows that (3.4) must be solved subject to

$$\psi_1 = -\frac{\psi_{0Y} (0, T)}{\sqrt{\mathrm{i}J}}, \quad Y = 0, \quad \psi_1 \to 0, \quad Y \to \infty. \tag{3.5}$$

The system (3.4)–(3.5) will only have a solution if a consistency condition is satisfied. This condition fixes $c_1 = c_1 (T)$ and, in general, c_1 will be complex. Thus, at any time T, there is an $O(R^{-1/2})$ viscous correction to the growth rate and wavespeed.

We note that the above discussion has not been dependent on the matter of whether or not there is a continuous spectrum at time T. However, it is trivial for us to locate

the continuous spectrum by matching exponentially small terms in our expansion procedure. We note that the exponentially decaying part of Ψ_1 will generate a rapidly decaying viscous term in the main part of the boundary layer. The viscous solutions of (2.1) for $Y = O(1)$ varying on a lengthscale $O(R^{-1/2})$ take the form

$$\psi = \exp \int^{Y} N(\widetilde{Y})\, \mathrm{d}\widetilde{Y}, \tag{3.6}$$

with

$$N^2 = \mathrm{i}\alpha R \left\{ u_B(Y, T) - c \right\}. \tag{3.7}$$

The branch of the square root is taken to match onto the exponentially decaying part of Ψ_1 and, since $N^2 \simeq -\mathrm{i}\alpha\sqrt{R}c_1$ for $Y \gg 1$, we find that ψ is ultimately oscillatory in the free stream when $-\mathrm{i}\alpha\sqrt{R}c_1$ is real and negative. This will not, in general, be the case, but if we now allow T to vary by an amount $O(R^{-1/2})$ and write

$$T = T^* = \overline{T}_0 + R^{-1/2}\overline{T} + \ldots \tag{3.8}$$

it follows that we have oscillatory behaviour of ψ for large Y if

$$\overline{T} = -\frac{c_{1R}(\overline{T})}{u_{BT}(\infty, \overline{T})}. \tag{3.9}$$

Hence, whenever an eigenvalue of (2.4) has $c_r = u_B(\infty, T)$, and $c_i < 0$ at $T = \overline{T}_0$ there is a time within $R^{-1/2}$ of $\overline{T}_0$ when the inviscid mode produces an oscillatory response in the free stream corresponding to a continuous spectrum. However, it follows from (3.6) that the oscillatory response in the free stream is of size $O(\exp(-QR^{1/2}))$ compared to ψ_0 where

$$Q = \left\{ \int_0^{\infty} \langle \mathrm{i}\alpha \left[u_B - c \right] \rangle^{1/2}\, \mathrm{d}Y \right\}_r. \tag{3.10}$$

This is in contrast to the situation at finite Reynolds numbers for steady boundary layers (e.g. Grosch & Salwen 1978), where the disturbance in the free stream and boundary layer are of comparable size.

Thus, at time T^*, the inviscid mode has an eigenfunction of size $O(1)$ in the main part of the boundary layer and an oscillatory tail of size $|\exp(-QR^{1/2})|$ outside the boundary layer.

Now let us contrast this behaviour with the form of the continuous spectrum eigenfunctions present at an arbitrary time T. We first note that, ψ_c, a decaying solution of (2.1) of the form given by (2.2), but with no boundary conditions imposed at $Y = 0$, can be found. In addition, two rapidly growing viscous modes of the form

$$\psi = \exp \int_0^{Y} N(\widetilde{Y})\, \mathrm{d}\widetilde{Y} \left\{ \widehat{\psi}_0 + \frac{1}{\sqrt{R}} \widehat{\psi}_1 + \ldots \right\}, \tag{3.11}$$

where N is given by (3.7) may be found. If we denote the exponentially growing and decaying solutions of this type by ψ_g and ψ_d and combine them with ψ_c to give

$$\psi = \psi_c + A\psi_g + B\psi_d,$$

then the constants A and B may be chosen such that $\psi = \psi_Y = 0$ and if $\psi_c \neq 0$, $Y = 0$, these constants will be $O(1)$. If c is chosen such that

$$c = u_B(\infty, T) - \mathrm{i}\lambda^2$$

where λ is a real contrast, then both solutions given by (3.11) are oscillatory at large Y, but ψ_g will be $O|\exp(R^{1/2}Q)|$. Thus, the continuous spectrum eigenfunction is concentrated outside the boundary layer, unlike the inviscid mode which crosses the continuous spectrum at $T = T^*$. It is for this reason that the mode remains distinct and exists either side of that interaction. This is in contrast with the corresponding behaviour at finite R. Finally, in this section, we point out that there is also the possibility of a continuous spectrum associated with disturbances not propagating in the free-stream direction. These modes are discussed in Shrira & Sazonov (2001) but are not relevant to the discussion here because the modes discussed here do not intersect with that continuous spectrum. The author wishes to thank one of the referees for making this observation.

4. Conclusions

Our investigation suggests there are no unstable Floquet modes of the Stokes layer stability problem at high Reynolds numbers. This suggests that for the neutral curve found by BB to exist, Reynolds numbers greater than about 700 must close at a higher value of R.

We have seen that if $\alpha_c > \alpha$, locally unstable non-Floquet modes originate from the viscous spectrum at times $T = \frac{1}{4}\pi + n\pi$ and cross the viscous continuous spectrum once quite soon after their birth. When $\alpha > \alpha_c$, the non-Floquet mode is generated at the same value of T, but no longer crosses the continuous spectrum. In fact, when $\alpha > \alpha_c$, the Floquet mode crosses the continuous spectrum. In a controlled experiment, the background disturbance level will be small, but we would expect that it will always be sufficiently large to stimulate the locally unstable inviscid mode with the largest growth rate. In an experiment, an obvious source for disturbances will be imperfections of the wall, so the modes which originate near the wall when the wall shear vanishes will be selectively stimulated. In addition free-stream disturbances can selectively stimulate the non-Floquet mode $\alpha_c > \alpha$ and the Floquet mode for $\alpha > \alpha_c$ at any time when the mode crosses the continuous spectrum. Of course, nonlinear effects will become important after sufficient linear growth and the present theory is no longer relevant. The lifetime growth G was shown in figure 8 as a function of α. We see that the mode with the maximum value of G is $\alpha \simeq 0.25$, so we would expect that this mode would be the one most likely to be observed experimentally. However, if the free-stream disturbances are the source of unstable modes which ultimately lead to transition, it is more instructive to compute the total growth of a mode once it has crossed the continuous spectrum. In fact, as shown in figure 8, there is virtually no difference in G computed from the birth of a mode and its intersection with the continuous spectrum. The different experimental investigations of the Stokes-layer problem have not reported the wavenumbers associated with local transition to turbulence, so we are unable to compare our predictions with experiment.

The author would like to thank the referees for their helpful comments on the first draft of this paper. Finally, we would like to thank Dr S. Cowley for some helpful discussions and Professors M. Hussaini and D. Furbish at Florida State University for their hospitality whilst part of this work was carried out.

REFERENCES

Blennerhassett, P. & Bassom, A. 2002 The linear stability of flat Stokes layers. *J. Fluid Mech.* **464**, 393–410 (referred to herein as BB).

Clamen, M. & Minton, P. 1977 An experimental investigation of flow in an oscillating pipe. *J. Fluid Mech.* **81**, 421–431.

Cowley, S. J. 1987 Stability of time dependent and spatially varying flows (ed. D. Dwoyer & M. Hussaini), pp. 261–275. Springer.

Grosch, C. & Salwen, H. 1978 Continuum spectrum of the Orr–Sommerfeld equation. *J. Fluid Mech.* **87**, 33–54.

Hall, P. 1978 The linear stability of flat Stokes layers. *Proc. R. Soc. Lond.* A**359**, 151–166.

Hall, P. 1983 The linear development of Görtler vortices in growing boundary layers. *J. Fluid Mech.* **130**, 41–58.

von Kerczek, C. & Davis, S. H. 1974 Linear stability theory of oscillatory Stokes layers. *J. Fluid Mech.* **62**, 753–773.

Seminara, G. & Hall, P. 1975 Centrifugal instability of a Stokes layer: linear theory. *Proc. R. Soc. Lond.* A**350**, 299–316.

Shrira, V. I. & Sazonov, I. A. 2001 Quasi-modes in boundary-layer-type flows. Part 1. Inviscid two-dimensional spatially harmonic perturbations. *J. Fluid Mech.* **446**, 133–171.

Tromans, P. S. 1979 Stability and transition in periodic pipe flows. PhD Thesis, Cambridge University, Engineering Dept.